Hazard Avoidance Products for Convectively-Induced Turbulence in Support of High-Altitude Global Hawk Aircraft Missions

Sarah M. Griffin and Christopher S. Velden
Cooperative Institute for Meteorological Satellite Studies, University of Wisconsin-Madison, Madison, WI

Abstract

A combination of satellite-based and ground-based information is used to identify regions of intense convection that may act as a hazard to high-altitude aircraft. Motivated by concerns that Global Hawk pilotless aircraft, flying near 60,000 feet, might encounter significant convectively-induced turbulence during research overflights of tropical cyclones, strict rules were put in place to avoid such hazards. However, these rules put constraints on science missions focused on sampling convection with on-board sensors.

To address these concerns, three hazard-avoidance tools to aid in real-time mission decision support are used to more precisely identify areas of potential turbulence: Satellite-derived Cloud-Top Height and Tropical Overshooting Tops, and ground-based global network lightning flashes. These tools are used to compare an ER-2 aircraft overflight of tropical cyclone Emily (2005), which experienced severe turbulence, to Global Hawk overflights of tropical cyclones Karl and Matthew (2010) that experienced no turbulence. It is found that the ER-2 overflew the lowest cloud tops and had the largest vertical separation from them compared to the Global Hawk flights. Therefore, cold cloud tops alone cannot predict turbulence. Unlike the overflights of Matthew and Karl, Emily exhibited multiple lightning flashes and a distinct overshooting top coincident with the observed turbulence. Therefore, these tools in tandem can better assist in identifying likely regions/periods of intense active convection. The primary outcome of this study is an altering of the Global Hawk overflight rules to be more flexible based on analyzed conditions.

1. Introduction

Given its flight range and cruising altitude of approximately 60 kft, the unmanned Global Hawk (GH) drone aircraft can provide an abundance of high altitude observations. These observations can be useful to atmospheric research and forecasting, especially when studying tropical cyclones (TCs) which can extend high into the upper-troposphere and even lower stratosphere, and often exist over the open-ocean hundreds of miles from the nearest conventional observations. TC forecasters and numerical model guidance can also benefit from real-time GH-provided information on storm structure, intensity and motion. For example, the data has been used to confirm the strengthening of TC Edouard (2014) over the open-Atlantic ocean (National Hurricane Center 2014) as well as the motion of TC Hermine (2016; National Hurricane Center 2016) near the Florida coast. Finally, high altitude observations also provide researchers with information on TC behavior and dynamics, such as data gathered during 27 flights over TCs as part of four different field experiments between 1998 and 2010 (Cecil et al. 2014). Two aircraft were utilized during these field experiments: the National Aeronautics and Space Administration (NASA) ER-2, a piloted aircraft that flies at approximately 65,000 ft (FL650), and the NASA unmanned GH.

Prior to the start of another research project in 2012 that utilized the GH, the NASA Hurricane and Severe Storm Sentinel (HS3) field experiment (Braun et al. 2016), new weather hazard avoidance rules were implemented for GH overflights of intense tropical convection (e.g., TCs). These rules included:

1. When flying below Flight Level (FL) 500 (50Kft in pressure altitude (PA) coordinates, 15.24 km), do not approach thunderstorms within 25 nautical miles

(nm).

2. When flying above FL500, do not approach reported lightning within 25 nm if cloud tops are at FL500 or higher. Aircraft should maintain at least 10,000 ft vertical separation from reported lightning if cloud tops are below FL500.
3. No overflight of cloud tops higher than FL500.

It is believed these rules were implemented as a result of an ER-2 flight over the center of TC Emily on 17 July 2005. The pilot encountered significant turbulence during an overpass of the TC eyewall, a ring of intense convection surrounding the TC center (American Meteorological Society 2015a). The turbulence encounter corresponded with an ER-2 Doppler radar (EDOP; Heymsfield et al. 2001) estimated updraft speed greater than 20 m s^{-1} (Cecil et al. 2010). Fig. 1 shows the GOES satellite infrared (IR) imagery from Emily (2005) and 1-h of the ER-2 flight track 1-h before and approximately during the time of the observed turbulence. Based on the IR brightness temperatures (BTs) alone, it is not immediately evident that the ER-2 would encounter turbulence in this case.

While the above rules were put into place to protect the GH from weather hazards such as turbulence, as the GH is not designed to fly in moderate or severe turbulence (Phil Hall, GH pilot, personal communication), high cloud tops are common in TCs (Houze 2010) and not always associated with turbulence. Therefore, these rules could put a constraint on obtaining valuable observations over a TC core. The purpose of this paper is to describe new hazard avoidance products that can be used toward mission decision-support to distinguish areas of possible high-altitude turbulence from areas that are safe for the GH to overfly. The outline is as follows: Section 2 describes the three elements of weather hazard avoidance developed to identify areas of high-altitude turbulence which are used in section 3 to compare the ER-2 overflight of TC Emily on 17 July 2005 with non-turbulent GH overflights of TC Karl and TC Matthew on 17 September 2010 and 24 September 2010, respectively. Section 4 outlines the modified GH flight rules resulting from the analysis in section 3, and section 5 provides some concluding remarks.

2. High-Altitude Weather Hazard Avoidance Products

Three specific products are described that, when utilized together, can be used to identify weather hazards for high-altitude aircraft missions in tropical regions. The products focus on deep vigorous convection that is not uncommon in the tropics, especially in TCs, and can be associated with aircraft hazards such as turbulence and lightning.

a. Very High Cloud Top Heights

Satellite-derived BTs based on IR imagery are often used as a proxy to identify areas of deep and active convection. However, cold IR BTs do not necessarily infer active convection. Other cloud properties need to be taken into account. For example, the cloud emissivity, optical depth, and type can be used to help discriminate convectively-active cumulonimbus from passive thick cirrus clouds. These properties can also be used to estimate the cloud top heights (CTH), which are more useful than the IR BTs for aviation purposes. CTH can be analyzed using most geostationary or polar-orbiting satellites.

This study utilizes IR imagery from the Geostationary Operational Environmental Satellite (GOES) satellite series (GOES 11-13) to calculate CTH. The first step involves the GOES-R Advanced Baseline Imager (ABI) Cloud Height Algorithm (ACHA; Heidinger 2011) that utilizes the IR BT data and a radiative transfer model to derive cloud-top temperatures (CTT). The CTTs are then converted to cloud-top pressures (CTP) using an atmospheric temperature profile provided by numerical weather prediction model data. The CTPs are then converted to CTH in pressure altitude (PA) coordinates using the method from Griffin et al. (2016). PA, the desired metric in the aviation community, is defined as the height of a given atmospheric pressure in the 1976 International Civil Aviation Organization standard atmosphere (American Meteorological Society 2015b).

As will be described in Section 3, the application of these CTH alone is not sufficient to detect hazardous regions to aviation. Very high-altitude CTH are one indicator of possible concerns, but additional information can augment the probabilities of encountering hazardous conditions.

b. Tropical Overshooting Tops

Detection of overshooting tops (OTs) in satellite imagery has been linked to vigorous updrafts and shown to correlate with severe weather and tropospheric turbulence (Bedka et al. 2010). The presence of these features above a high cirrus cloud canopy can be a distinguishing feature for determining areas of active convection vs. quiescent conditions at high-altitude flight levels. Tropical overshooting tops (TOTs) can be identified using an objective satellite-based detection algorithm (Monette et al. 2012), which is a derivative of an OT detection algorithm developed by Bedka et al. (2010). TOTs are identified as pixels colder than 215 K in the GOES 10.7-μm IR BTs. The mean BT of the anvil cloud surrounding each TOT candidate pixel is computed using pixels at an 8 km radius in 16 radial directions. At least 9-of-16 anvil pixels must have a BT colder than 225 K, and only these pixels are used to calculate the mean anvil BT. TOT strength can be defined using the BT difference (BTD) between the coldest TOT pixel and the mean anvil BT. Candidate TOTs are divided into two categories based on their BTDs: those with a BTD less than or equal to -9 K and those with a BTD greater than -9 K, based on Monette et al. (2012). For application to TCs, TOTs with a BTD greater than -9 K are only identified within 100 km of the TC center, where the coldest cloud tops associated with the central dense overcast are more prevalent (Velden et al. 1998). Further information about the TOT algorithm can be found in Griffin (2017).

c. Lightning

Electrical activity in clouds is another sign of active convection. Lightning can be detected using ground-based networks such as the Vaisala Long-range Lightning Detection Network (LLDN). The LLDN uses the large electromagnetic signals associated with cloud-to-ground lightning return strokes, as well as large pulses in cloud discharges, to identify the timing and location of lightning discharges using as few as two sensors. The LLDN employs a subset of the approximately 200 sensors from the United States (US) National Lightning Detection Network and the Canadian Lightning Detection Network (Cummins et al. 2008).

The accuracy of LLDN lightning data can be described using the detection efficiency and location accuracy. The detection efficiency over the Atlantic Ocean is shown in Fig. 2, adapted from Pessi et al. (2009). Detection efficiency is highest near the US coastline and decreases with increasing distance from land. For a given location, the detection efficiency during the day, which is defined as between 12 UTC and 22 UTC, is lower than during the night, defined as 00 UTC to 10 UTC. Location accuracy is about 1 km near the US coast, falling off uniformly to about 30 km near the 5% detection efficiency boundary. More information about the Vaisala LLDN can be found in Pessi et al. (2009). Improved coverage over oceanic regions is becoming available from new satellite-based instruments, such as the GOES-R Lightning Mapper.

3. Comparison of TC Overflight Cases

In this section we utilize the products described above to characterize and compare selected overflights of TCs by high-altitude aircraft. During TC Emily (2005), a NASA ER-2 overflew the storm as part of a research mission, and encountered severe turbulence noted by the pilot. In 2010, two TCs (Karl and Matthew) were overflown by the GH as part of a research campaign, and in neither case was any turbulence detected by the pilotless aircraft.

a. Cloud Top Heights

The CTH during the three flights are analyzed using GOES-11 imagery for Emily and GOES-13 imagery for Karl and Matthew. The ACHA CTH products for these three overflights were not available in real-time, and have been post-processed for this study. Fig. 3 illustrates the vertical cross-sections of each flight. The solid black lines represent the aircraft height during flight, with the gray curtain underneath them representing the 10,000 ft ‘safety’ barrier outlined in the second GH flight rule noted previously. The dashed black lines represent FL500, the maximum CTH that overflights should be allowed to occur based on a strict enforcement of the third GH flight rule. The small squares represent the CTH values closest to (within 10 km and 30 seconds) the aircraft location and time. The square colors represent the cloud emissivity, with higher emissivity representing thicker clouds.

Taken on face value, Fig. 3 indicates that multiple violations of the GH flight rules outlined in section 1 occurred during these three overflights. On all three overflights, the aircraft flew over CTHs higher than FL500, violating the third GH flight rule. The highest cloud tops, at a pressure altitude of approximately 56,800 ft, were overflown during the GH overflight of TC Matthew (Fig 3c). The GH also overflew CTH of approximately 54,800 ft over TC Karl (Fig. 3b). In comparison, when turbulence was observed during the overflight of TC Emily (Fig 3a), the maximum CTHs were approximately 54,200 ft. In addition, all aircraft flew within 10,000 ft vertical separation of the CTH, violating the second GH flight rule. The GH flew the closest to the CTH over TC Karl (Fig 3b), at one point with only a ~2350 ft vertical separation. The GH minimum vertical separation from the CTH of TC Matthew was about 4500 ft. The ER-2 maintained the largest minimum vertical separation from the CTH of ~9600 ft. Yet, the ER-2 experienced turbulence strong enough for the pilot to deem the mission plan unsafe (Cecil et al. 2010), while the GH did not encounter any noteworthy turbulence. Therefore, CTH alone cannot be used to distinguish high-altitude areas of turbulence from areas that are safe to overfly.

b. Tropical Overshooting Tops (TOTs) and Lightning

Since the CTH alone cannot distinguish potential flight hazards, two additional products are utilized: cloud overshooting tops and lightning. Overshooting tops are a known cause of convectively-induced turbulence (Bedka et. al 2010), with the probability of experiencing moderate or greater turbulence increasing as distance from the overshooting top decreases. This turbulence is potentially caused by thunderstorm updrafts generating vertically propagating gravity waves (Fovell et al. 1992, Lane et al. 2012). TOT BTD can be used as a proxy for updraft strength. As seen in Fig. 4, TOT BTD is moderately correlated to the maximum updraft speed identified by the ER-2 Doppler Radar (Heymsfield et al. 2010). The occurrence of lightning is also indicative of intense convection (Carey and Rutledge 2000) and has been correlated with reported aircraft turbulence (Wolff and Sharman 2008). For applications to high-altitude flights over tropical areas, especially oceanic, TOTs and lightning data can be used to supplement the CTH information to better inform on potential flight hazards.

The CTH, TOTs, and lightning for the approximate time the ER-2 observed turbulence over TC Emily can be seen in Fig. 5. For this example the CTH and TOTs are identified using GOES-12 instead of GOES-11, as GOES-12 provides a better viewing angle of TC Emily compared to GOES-11. GOES-11 was used for the plots in Fig. 3 as it was in rapid-scan mode with 5-minute temporal resolution compared to 15-min temporal resolution for GOES-12. TOTs are represented by pink symbols, with the shape of each symbol indicating the magnitude of the TOT. Larger magnitude TOTSs can be associated with stronger updrafts (Monette et al. 2014), potentially increasing the possibility of experiencing turbulence. Lightning flashes are represented by cyan crosses, with the most recent flashes indicated by larger crosses. Lightning flashes are defined as the average location of all lightning strokes within 75 km and 1 second of each other. At the time of observed turbulence, the ER-2 is in the vicinity of a small area of high CTH in the inner northwest eyewall and an associated TOT with a large magnitude (BTD of 11.74 K) commensurate with an aircraft-measured updraft of 23.5 m s^{-1} (Heymsfield et al. 2010).

In addition, multiple lightning flashes are observed near the TOT, further indicating active convection in the vicinity of the ER-2 when turbulence was experienced.

As a comparison with Fig. 5, Fig. 6 depicts the CTH, TOTs, and lightning from the GH overflights of TC Matthew and TC Karl when no turbulence was experienced. Fig. 6a is coincident with the GH overflying some of the highest CTHs observed in TC Matthew. Unlike the ER-2 over TC Emily in Fig. 5, no TOTs or lightning is observed in the vicinity of the GH track. So, while the CTHs are very high, they could be the result of dense cirrus outflow from previous convection in this region that was indicated around 05 UTC (not shown) (McFarquhar and Heymsfield 1997). Fig. 6b depicts TC Karl during the GH's smallest vertical separation from the CTH. Once again, high CTH but no TOTs are observed in the vicinity during this GH overflight. A few lightning flashes are observed, however the flashes are fewer in number and older than the lightning flashes observed in TC Emily (the lightning network detection efficiency for both TC Emily and TC Karl was approximately 30%). Therefore, these cases indicate that all three products, best used in tandem, are essential for identifying areas of vigorous convection which could potentially cause hazardous conditions for high-altitude aircraft.

4. Update to GH flight rules

As a result of the above analysis, the existing GH flight rules were amended to somewhat relax the restrictions on overflying TCs with very high CTH. The updated flight rules allow overflights if no significant convective overshoots or frequent lightning is observed, essentially removing the rule advising against the overflight of CTH higher than FL500. A 25 nm spatial separation between the GH and TOTs/frequent lightning is still advised, or at least 10,000 ft vertical separation is to be maintained, if the CTH is below FL500 and the GH is above FL500. However, if the CTH is above FL500 and TOTs but no lightning is observed, only a 5,000 ft vertical separation is necessary. The GH is clear to overfly CTHs below FL500 with TOTs but no frequent lightning.

These modified rules were in place during more recent TC field programs that employed the GH for high-altitude data collection. The remote pilots had access to the three aforementioned products in real-time, with updates every 1-30 minutes depending on the product and available scanning frequency. Some real-time examples from the NASA HS3 and the National Oceanic and Atmospheric Administration (NOAA) Sensing Hazards with Operational Unmanned Technology (SHOUT) GH overflights of TCs are shown in Figs. 6 and 7. A good example of GH hazard avoidance occurred during the overflight of TC Dolly as part of an HS3 mission. Fig. 7 shows that the GH overflies CTH above FL520 where no TOTs are observed, however it turns away from the region associated with very high CTH and frequent lightning. Fig. 8 depicts the GH overflight of TC Matthew in 2016 during SHOUT. While the CTH associated with TC Matthew was very high (around FL580), neither TOTs nor lightning was observed, and no turbulence was reported.

5. Discussion and Conclusions

This study explores the use of satellite and lightning products to improve the analysis of conditions for high altitude (~60kft) aircraft during overflights of tropical cyclones (TCs). Three primary tools are identified: Cloud-Top Heights (CTH), Tropical Overshooting Tops (TOTs), and lightning data. CTH and TOTs are identified using geostationary satellite algorithms, while lightning is detected using the Vaisala Long-range Lightning Detection Network. In the case studies examined (and other experiences based on real-time applications), it is found that no product by itself is an adequate predictor of high-altitude flight hazards. However, a combination of all three products when viewed together can convincingly identify likely regions/periods of intense convection in TCs with possible associated above-cloud turbulence vs. quasi-undisturbed conditions.

The motivation for this study was to re-examine existing GH flight rules that were thought to be too strict during the 2012 field phase of the NASA HS3 experiment. Based on these rules, GH overflights of TCs were somewhat restricted, potentially limiting the usefulness of the experiment. However, later in HS3 a few flight legs were allowed over very high CTH if no concurrent TOTs or lightning was observed. Detectors onboard the GH indicated no significant turbulence during these overflights.

The origin of the flight rules is believed to have come from a single ER-2 overflight of TC Emily (2005) that experienced severe turbulence when overflying a convective updraft of at least 20 m s^{-1}. The conditions associated with the turbulent ER-2 overflight of TC Emily are compared to the GH overflights of TCs Matthew and Karl in 2010 that did not experience noteworthy turbulence. Significant findings include:

1. The CTH of the convective cell in TC Emily's eyewall overflown at the time of the observed turbulence was lower than most of the high CTH overflown by the GH during TCs Matthew and Karl. Therefore, cold IR brightness temperatures or high CTH are a not sufficient condition for restricted flight paths.
2. The vertical separation between the ER-2 and TC Emily's CTH at the time of the observed turbulence was larger than the minimum vertical separation between the GH and the highest CTH from TCs Karl and Matthew. If the cloud tops appear

non-convective and no lightning is observed, then a smaller "safe zone" above the clouds can be allowed.

3. At the approximate time and location of the ER-2 turbulence report during TC Emily, a strong TOT was detected along with multiple lightning flashes that were coincident with a strong convective updraft. No TOTs or lightning flashes were detected during the GH overflight of the highest CTH in TC Matthew, and no TOTs and only a few older lightning flashes were observed during the GH minimum vertical separation from the CTH over TC Karl.

Therefore, it is concluded that all three products should be used together to best identify areas of potential turbulence resulting from TC convection.

As a result of this study, the GH flight rules were modified to lift the maximum CTH constraint if TOTs and lightning flashes are not detected. However, vertical and horizontal separation from active convection (e.g. TOTs) should still be maintained. These modified rules allowed for many successful overflights of multiple TCs during the subsequent HS3 and SHOUT campaigns.

The real-time CTH and TOT products for Atlantic and Eastern Pacific GH missions are currently being provided by the Cooperative Institute for Meteorological Satellite Studies at the University of Wisconsin on an experimental basis. The lightning data is provided by the Unidata Global Lightning Network. In the future, the ACHA CTH will become an operational GOES product at NOAA/NESDIS. At this time, the TOT product is not on an operational track at NOAA/NESDIS, but will be continued to be supported by CIMSS for specific applications. The coverage of lightning data over the tropical Atlantic and eastern Pacific will expand with the deployment of the Lightning

Mapper on the GOES-R series of geostationary satellites. Therefore it will be possible to expand the research and findings of this study to more general transoceanic aviation applications.

Acknowledgements

The authors wish to acknowledge the encouragement of several individuals to the advancement of this work: Ed Zipser, Scott Braun, Dan Cecil, Gerald Heymsfield, Jason Dunion, Gary Wick, Peter Black, Kris Bedka, Andy Heidinger, Wayne Feltz, Amber Emory. Support for this research was provided by the following programs: NASA HS3, NOAA GOES-R Risk Reduction, and NOAA SHOUT.

References

American Meteorological Society (2015a). “Eyewall” Glossary of Meteorology. http://glossary.ametsoc.org/wiki/ Eyewall. Accessed 13 June 2017.

American Meteorological Society (2015b). “Pressure Altitude” Glossary of Meteorology. http://glossary.ametsoc.org/wiki/Pressure_altitude. Accessed 13 June 2017.

Bedka, K. M., Brunner, J., Dworak, R., Feltz, W., Otkin, J., Greenwald, T., (2010). Objective Satellite-Based Overshooting Top Detection Using Infrared Window Channel Brightness Temperature Gradients. *J. Appl. Meteor. And Climatol.*, **49**, 181-202.

Braun, S. A., P. A. Newman, P. A., Heymsfield, G.M. (2016). NASA’s Hurricane and Severe Storm Sentinel (HS3) investigation. *Bull. Amer. Meteor. Soc.*, **97**, 2085–2102.

Carey, L. D. and Rutledge, S. A., (2000). The relationship between precipitation and lightning in tropical island convection: A C-band polarimetric radar study. *Mon. Wea. Rev.*, **128**, 2687–2710.

Cecil, D. J., Quinlan, K. R., Mach, D. M. (2010). Intense convection observed by NASA ER-2 in Hurricane Emily (2005). *Mon. Wea. Rev.*, **138**, 765–780.

________, Zipser, R. J., Velden, C. S., Monette, S. A., Heymsfield, G. M., Braun, S. A., Newman, P. A., Black, P. G., Black, M. L., Dunion, J. P., (2014). Weather Avoidance

Guidelines for NASA Global Hawk High‐ Altitude Unmanned Aircraft Systems (UAS). National Aeronautics and Space Administration. https://ntrs.nasa.gov/archive/nasa/casi.ntrs.nasa.gov/20140008781.pdf. Accessed 13 June 2017.

Cummins, K. L., Murphy, M. J., Demetriades, N. W. S., Pifer, B., Pessi, A., Businger, S., (2008). Modeling and calibration of Vaisala's operational long range lightning detection network. *20th International Lightning Detection Conference*, USA, Tucson AZ, 2008. https://pdfs.semanticscholar.org/79a5/9df76ae1f95caf631470a52d49553490e4c3.pdf. Accessed 13 June 2017.

Fovell, R., D. Durran, and J. R. Holton (1992), Numerical simulations of convectively generated stratospheric gravity waves, *J. Atmos. Sci.*, **49**, 1427–1442.

Griffin, S. M., (2017). Climatology of Tropical Overshooting Tops in North Atlantic Tropical Cyclones. *J. Appl. Meteor. Climatol*, **56**, 1783-1796.

___________, Bedka, K. M., Velden, C. S., (2016). A method for calculating the height of overshooting convective cloud tops using satellite-based IR imager and CloudSat cloud profiling radar observations. *J. Appl. Meteor. Climatol.*, **55**, 479–491.

Heidinger, A. K., (2011). ABI cloud height. NOAA NESDIS Center for Satellite Applications and Research Algorithm Theoretical Basis Doc. http://www.goes-r.gov/products/ATBDs/baseline/Cloud_CldHeight_v2.0_no_color. pdf. Accessed 13 July 2017.

Heymsfield, G. M., Halverson, J. B., Simpson, J., Tian, L., Bui, T. P., (2001). ER-2 Doppler radar investigations of the eyewall of Hurricane Bonnie during the Convection and Moisture Experiment-3. *J. Appl. Meteor.*, **40**, 1310–1330.

___________, Tian, L., Heymsfield, A.J., Li, L., and Guimond, S. (2010). Characteristics of deep tropical and subtropical convection from nadir-viewing high-altitude airborne Doppler radar. *J. Atmos. Sci.*, **67**, 285–308.

Houze, R. A., Jr., (2010). Clouds in tropical cyclones. *Mon. Wea. Rev.*, **138**, 293–344.

Lane, T. P., R. D. Sharman, St. B. Trier, R. G. Fovell, and J. K. Williams, 2012: Recent advances in the understanding of near- cloud turbulence. *Bull. Amer. Meteor. Soc.*, **93**, 499–515.

McFarquhar, G. M. and A. J. Heymsfield, A.J. (1997). Parameterization of tropical cirrus ice crystal size distributions and implications for radiative transfer: Results from CEPEX. *J. Atmos. Sci.*, **54**, 2187–2200 .

Monette, S. A., Velden, C. S., Griffin, K. S., Rozoff C. M., (2012). Examining trends in satellite-detected tropical overshooting tops as a potential predictor of tropical cyclone rapid intensification. *J. Appl. Meteor. Climatol.*, **51**, 1917–1930.

___________, ___________, Zipser, E. J., Cecil, D. J., Black, P. G., Braun, S. A. and Heymsfield, G. M. (2014). Differentiating Tropical Cyclones Exhibiting Strong Updrafts using Combined Satellite, Lightning, and Global Hawk Observations. *31st Conference on Hurricanes and Tropical Meteorology*, USA, San Diego, CA. https://ams.confex.com/ams/31Hurr/videogateway.cgi/id/26889?recordingid=26889

National Hurricane Center (2014). Hurricane Edouard Discussion 16. http://www.nhc.noaa.gov/archive/2014/al06/al062014.discus.016.shtml. Accessed 28 July 2017.

___________ (2016). Tropical Storm Hermine Discussion 16. http://www.nhc.noaa.gov/archive/2016/al09/al092016.discus.016.shtml. Accessed 28 July 2017.

Pessi, A. T., S. Businger, S., K. L. Cummins, *K. L.*, Demetriades, N. W. S., Murphy, M., and B. Pifer (2009), Development of a long-range lightning detection network for the Pacific: Construction, calibration, and performance, *J. Atmos. Oceanic Technol.*, **26**, 145–166.

Velden, C. S., T. L. Olander, and R. M. Zehr (1998). Development of an objective scheme to estimate tropical cyclone intensity from digital geostationary satellite infrared imagery. *Wea. Forecasting*, **13**, 172–186.

Wolff, J. K. and Sharman, R. (2008). Climatology of upper-level turbulence over the contiguous United States. *J. Appl. Meteor. Climatol.*, **47**, 2198–2214.

List of Figures

Fig. 1. Satellite infrared (IR) imagery from TC Emily (2005) and previous hour of the ER-2 flight track at approximately the time of the observed turbulence, 0750 UTC on 17 July 2005.

Fig. 2. Vaisala Long-range Lightning Detection Network detection efficiency for both day (12 UTC to 22 UTC) and night (00 UTC to 10 UTC). Adapted from Pessi et al. (2009).

Fig. 3. Vertical cross-section of CTH and aircraft height for the overflights of a) TC Emily (2005), b) TC Karl (2010), and c) TC Matthew (2010). The solid black line and gray curtain underneath represents the aircraft height and 10,000 ft vertical separation, respectively. The small squares represent the CTH derived from GOES coincident with the aircraft location and time, colored by cloud emissivity (thickness).

Fig. 4. Correlation between TOT brightness temperature difference and ER-2 Doppler Radar (EDOP) measured maximum updraft speed from 13 TC updrafts.

Fig. 5. ER-2 flight track height and CTH, TOTs, and lightning from 17 July 2005 at 0745 UTC for the overflight of TC Emily, with the plane symbol located at the approximate location turbulence was experienced.

Fig. 6. GH flight track height and CTH, TOTs, and lightning from (a) 24 September 2010 at 0815 UTC during the overflight of TC Matthew and (b) 16 September 2010 at 2115 UTC during the overflight of TC Karl. Fig. 6a depicts the time of highest CTH overflown by the GH, and Fig. 6b depicts the time of minimum vertical separation between the GH and CTH.

Fig. 7. GH flight track height, TOTs and lightning from 2 September 2014 at 2150 UTC for the overflight of TC Dolly. CTH and TOTs are from 2 September 2014 at 2130 UTC.

Fig. 8. GH flight track height, TOTs and lightning from 7 October 2016 at 1204 UTC for the overflight of TC Matthew. CTH and TOTs are from 7 October 2016 at 1145 UTC.

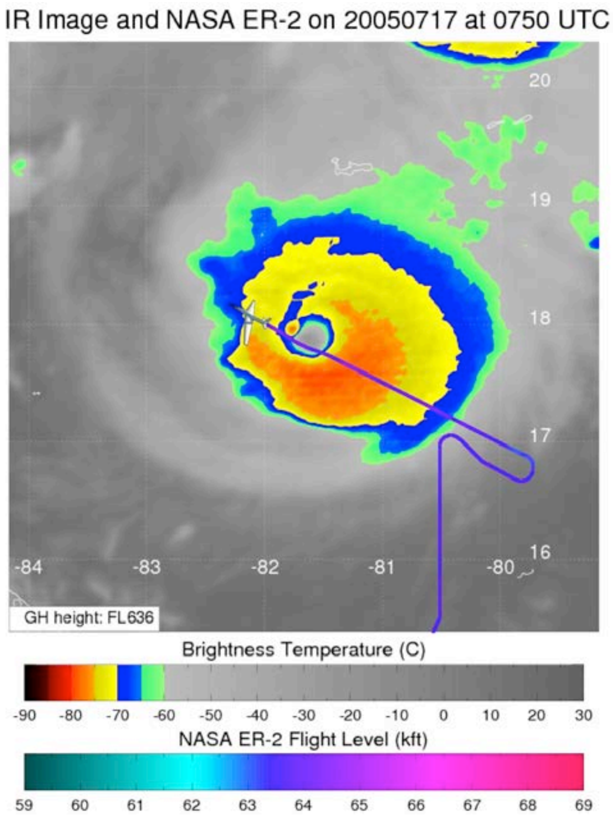

Fig. 1. Satellite infrared (IR) imagery from TC Emily (2005) and previous hour of the ER-2 flight track at approximately the time of the observed turbulence, 0750 UTC on 17 July 2005.

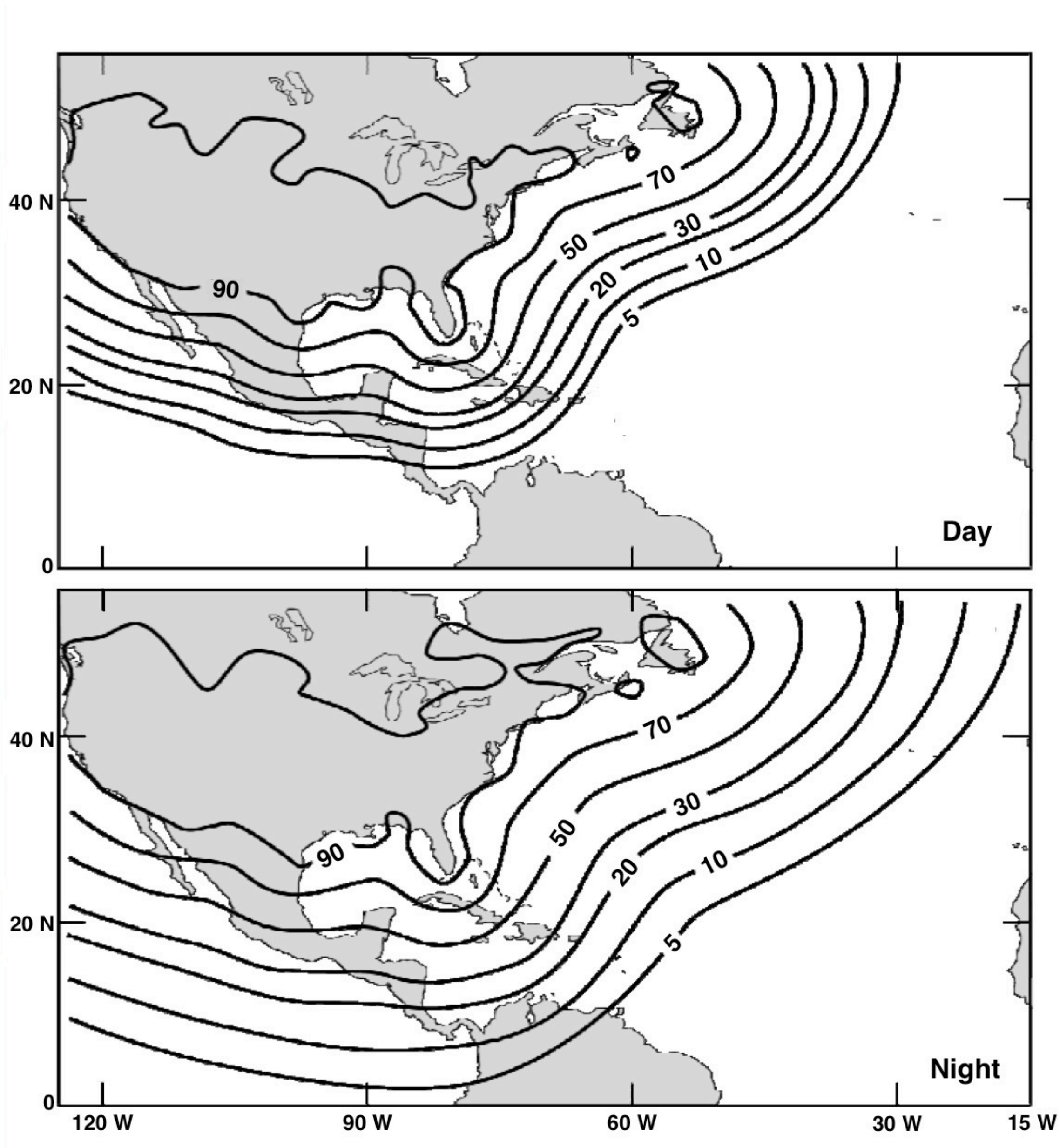

Fig. 2. Vaisala Long-range Lightning Detection Network detection efficiency for both day (12 UTC to 22 UTC) and night (00 UTC to 10 UTC). Adapted from Pessi et al. (2009).

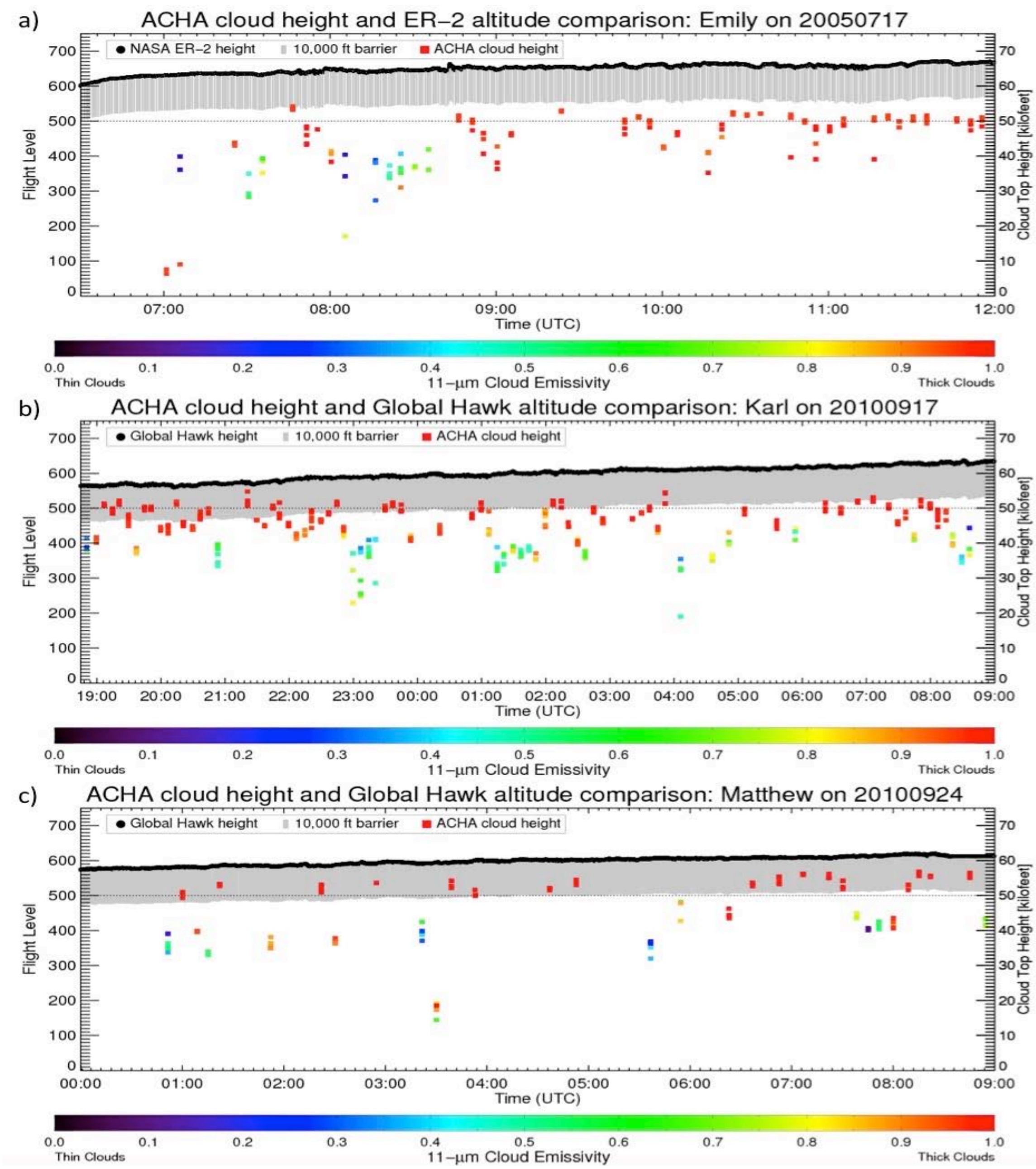

Fig. 3. Vertical cross-section of CTH and aircraft height for the overflights of a) TC Emily (2005), b) TC Karl (2010), and c) TC Matthew (2010). The solid black line and gray curtain underneath represents the aircraft height and 10,000 ft vertical separation, respectively. The small squares represent the CTH derived from GOES coincident with the aircraft location and time, colored by cloud emissivity (thickness).

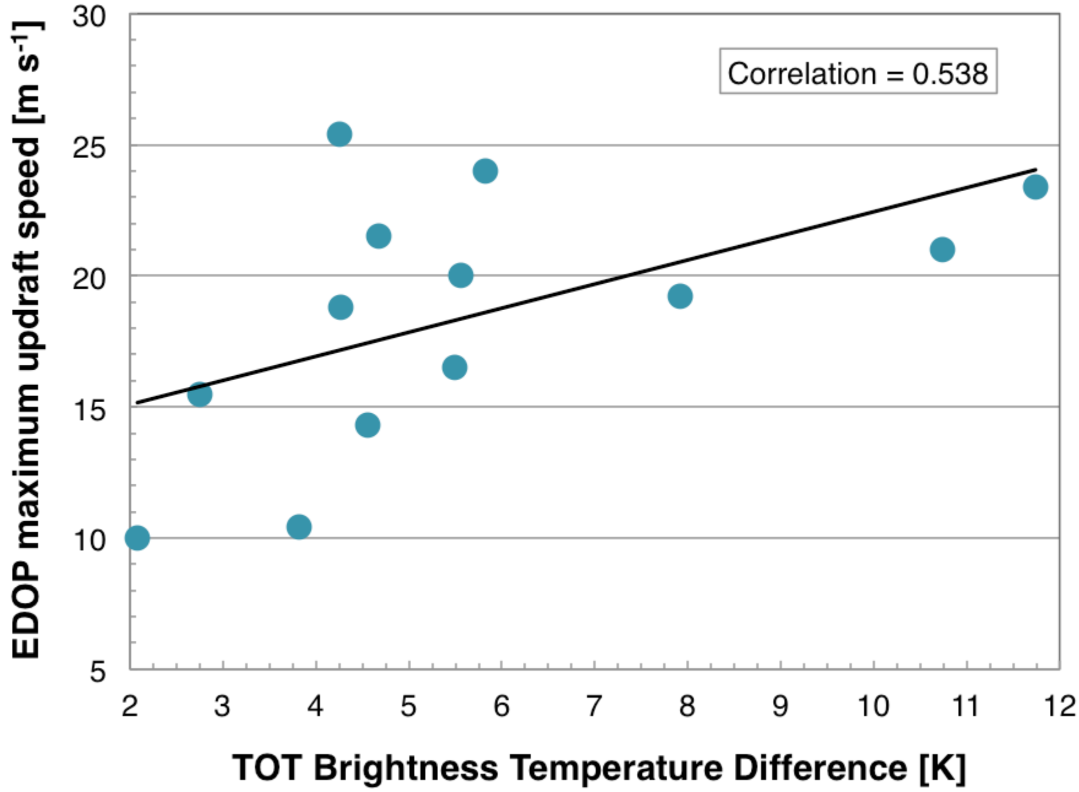

Fig. 4. Correlation between TOT brightness temperature difference and ER-2 Doppler Radar (EDOP) measured maximum updraft speed from 13 TC updrafts.

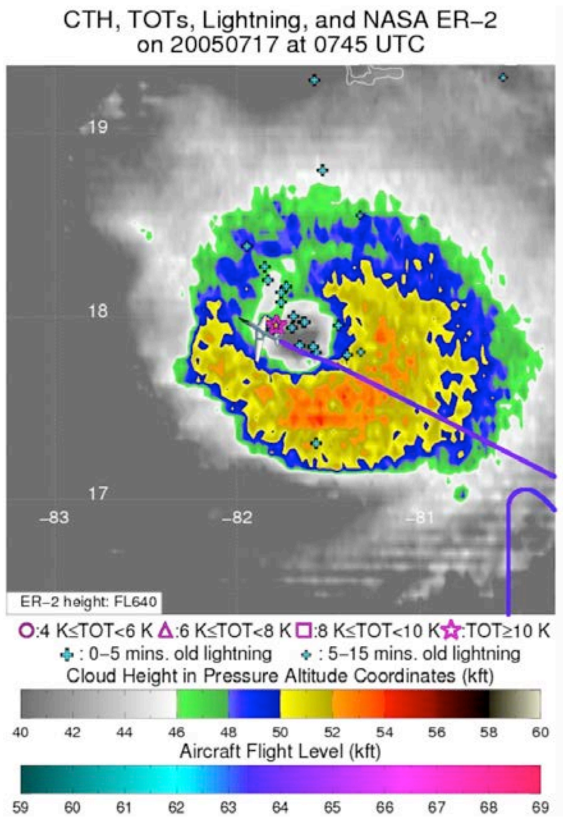

Fig. 5. ER-2 flight track height and CTH, TOTs, and lightning from 17 July 2005 at 0745 UTC for the overflight of TC Emily, with the plane symbol located at the approximate location turbulence was experienced.

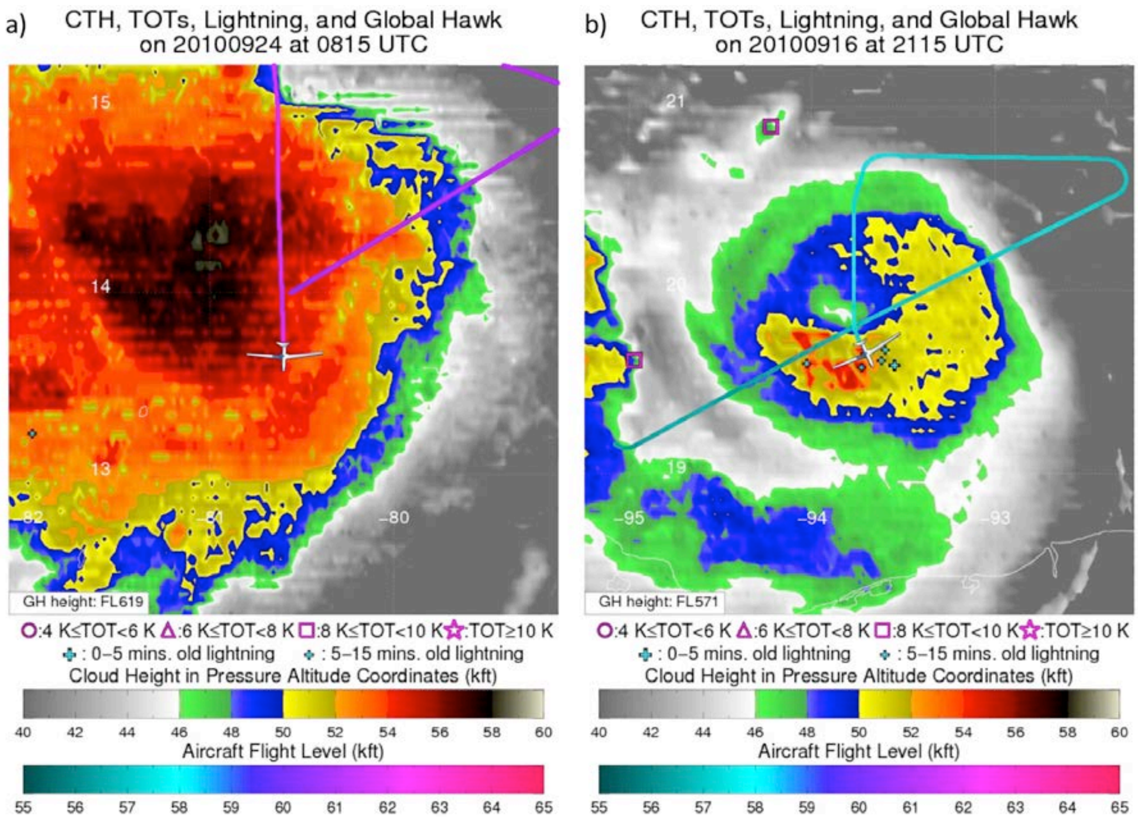

Fig. 6. GH flight track height and CTH, TOTs, and lightning from (a) 24 September 2010 at 0815 UTC during the overflight of TC Matthew and (b) 16 September 2010 at 2115 UTC during the overflight of TC Karl. Fig. 6a depicts the time of highest CTH overflown by the GH, and Fig. 6b depicts the time of minimum vertical separation between the GH and CTH.

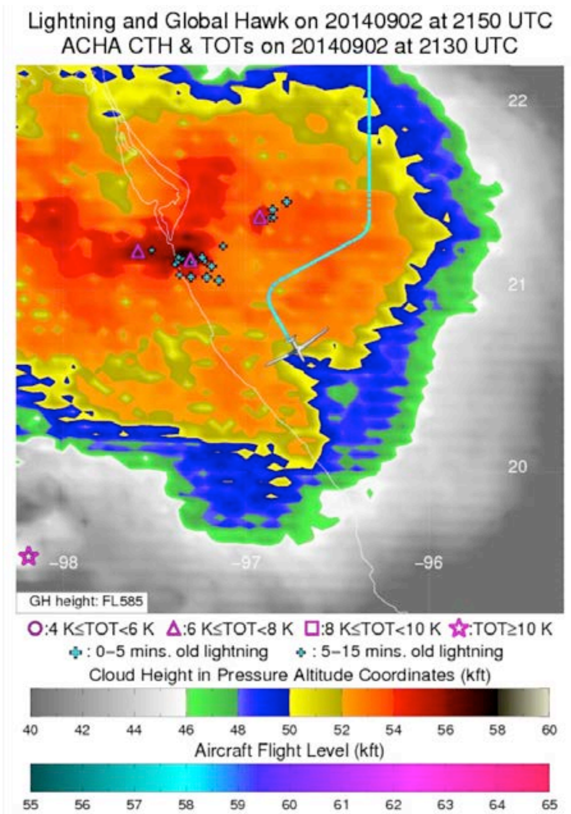

Fig. 7. GH flight track height, TOTs and lightning from 2 September 2014 at 2150 UTC for the overflight of TC Dolly. CTH and TOTs are from 2 September 2014 at 2130 UTC.

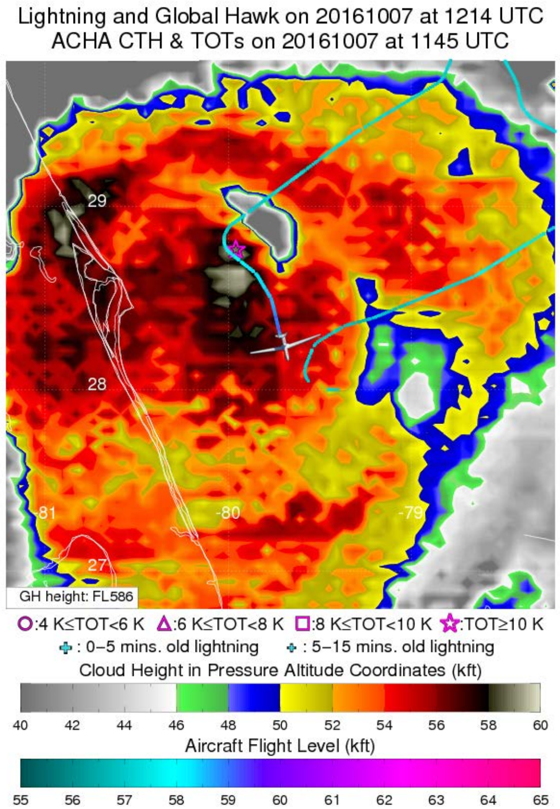

Fig. 8. GH flight track height, TOTs and lightning from 7 October 2016 at 1204 UTC for the overflight of TC Matthew. CTH and TOTs are from 7 October 2016 at 1145 UTC.